

Zeolites | Hot Paper |

 Synthesis and Structure Determination of SCM-15: A 3D Large Pore Zeolite with Interconnected Straight 12 × 12 × 10-Ring ChannelsYi Luo,^[a, b, c] Stef Smeets,^[b] Zhendong Wang,^{*,[a]} Junliang Sun,^{*,[b, c]} and Weimin Yang^{*,[a]}

Abstract: A new germanosilicate zeolite named SCM-15 (Sinopec Composite Material No. 15), the first zeolite containing a 3-dimensional (3D) channel system with interconnected 12-, 12-, and 10-ring channels (pore sizes: 6.1 × 7.2, 6.1 × 7.4, and 5.2 × 5.9 Å), has been synthesized using neutral 4-pyrrolidinopyridine as organic structure-directing agents (OSDAs). Its structure has been determined by combining single-crystal electron diffraction (SCED) and synchrotron powder X-ray diffraction (SPXD) data. The unique open framework structure of SCM-15 is related to that of FOS-5 (BEC), ITQ-7 (ISV), PKU-16 (POS), ITQ-26 (IWS), ITQ-21, Beta polymorph B, and SU-78B, since all these framework structures can be constructed from similar chains which are connected through shared 4-ring or double 4-ring (*d4r*) units. Based on this relation, six topologically reasonable 3D large or extra-large pore hypothetical zeolites are predicted.

Zeolites are an important class of crystalline microporous materials with molecular-scale pore architectures, tunable chemical compositions, and various morphologies. These outstanding characteristics have endowed zeolites with excellent properties in catalysis, gas adsorption/separation, and ion-exchange applications.^[1–4] The macroscopic properties of a zeolite in these applications rely primarily on its microscopic structure features, especially the size of the pores and the dimensionality of the channel system.^[5] Currently, among all available zeolites, the most successful ones are those containing either 3D

large (12 × 12 × 12-ring) or medium (10 × 10 × 10-ring) pores channel systems such as zeolite Y (FAU), Beta (*BEA), and ZSM-5 (MFI). These zeolites have been widely applied in various industrial processes, because of their excellent capability for the diffusion of different molecules and the possibility to induce different product selectivities based on their pore architectures and chemical compositions.^[6] In this sense, zeolites with mixed large and medium pores are of particular interest because they may combine some of the same properties of large and medium pore zeolites.^[7,8] Many efforts therefore have been made in the synthesis of zeolites with novel 3D interconnected large and medium pore channel systems (i.e. 12 × 10 × 10-ring or 12 × 12 × 10-ring). CIT-1 (CON) is the first material reported containing a channel system with interconnected large and medium pores (12 × 10 × 10-ring) that provide molecular access to the crystal interior through both type of pores.^[8] The channel system of CON is constructed by straight 12-ring channels that are perpendicular to straight and bending 10-ring channels.^[8,9] A related framework type, IWR also possesses the same 3D 12 × 10 × 10-ring channel system as that of CON.^[10] Later on, a series of interesting zeolites (such as ITG, *-ITN and MSE) with interconnected large and medium pores have been synthesized.^[7,11–15] However, the 3D channel systems of these framework types are all 12 × 10 × 10-ring, and zeolites with more open 3D interconnected 12 × 12 × 10-ring channels have not yet been reported.


Recently, we have reported the synthesis of SCM-14 (SOR), a new large pore germanosilicate zeolite synthesized using neutral 4-pyrrolidinopyridine as organic structure-directing agents (OSDAs) in fluoride medium.^[16] In this work, we present the synthesis of SCM-15, using the same OSDA. To the extent of our knowledge, it is the first large pore zeolite consisting of interconnected 12 × 12 × 10-ring channels. Its structure was initially determined using single-crystal electron diffraction (SCED), and refined using synchrotron powder X-ray diffraction (SPXD) data.^[17] The framework structure of SCM-15 is related to that of FOS-5 (BEC), ITQ-7 (ISV), PKU-16 (POS), ITQ-26 (IWS), ITQ-21, Beta polymorph B, and SU-78B,^[18–24] since this class of framework structures can all be built from similar chains which are connected by shared 4-ring or *d4r* units and the chains themselves are also built from similar or the same building units. Based on the structure relationship between these frameworks, six hypothetical zeolites were predicted.

SCM-15 zeolites with a needle-like morphology were synthesized using the same OSDA as that used for the synthesis of SCM-14 (SOR) in the presence of Ge and F[−] (Figure S1). During

[a] Dr. Y. Luo, Dr. Z. Wang, Prof. W. Yang
State Key Laboratory of Green Chemical Engineering and Industrial Catalysis
Sinopec Shanghai Research Institute of Petrochemical Technology
1658 Pudong Beilu, Shanghai 201208 (China)
E-mail: wangzd.sshy@sinopec.com
yangwm.sshy@sinopec.com

[b] Dr. Y. Luo, Dr. S. Smeets, Prof. J. Sun
Department of Materials and Environmental Chemistry
Stockholm University, SE-106 91 Stockholm (Sweden)
E-mail: junliang.sun@pku.edu.cn

[c] Dr. Y. Luo, Prof. J. Sun
College of Chemistry & Molecular Engineering
Peking University, No.5 Yiheyuan Road, Beijing 100871 (China)

 Supporting information and the ORCID identification number(s) for the author(s) of this article can be found under:
<https://doi.org/10.1002/chem.201805187>.

the crystallization, a noticeable amount of an SCM-14 phase always appeared in the products of SCM-15. The most pure product of SCM-15 with a trace amount of SCM-14 and amorphous was prepared using an optimized gel molar composition and is described in the experimental section.

Elemental analysis and ^{13}C solid-state MAS NMR spectroscopy of as-made SCM-15 demonstrate that the OSDA molecules remain intact within the framework structure (Table S1, Figure S2). Besides, the ^{13}C liquid NMR spectra of protonated OSDA molecules in solution with different pH values coupled with the pH value ($\approx 8\text{--}9$) of the starting gel reveal that the OSDA molecules in the structure of SCM-15 are mainly mono-protonated and charge-balanced by F^- ions (Figure S2). The ^{19}F MAS NMR spectrum of as-made SCM-15 indicates the F^- ions are located in the small $d4r$ units, since two resonance bands centered at -7.7 and -18.9 ppm are present in the spectrum (Figure S3). Previous studies have shown that the band at -18.9 ppm can be attributed to the F^- ions located in the $d4r$ units containing isolated Ge atoms, which may mainly correspond to $d4r$ units with a composition of $\text{Si}_{6.0}\text{Ge}_{2.0}$ or $\text{Si}_{7.0}\text{Ge}_{1.0}$. The band at -7.7 ppm can be ascribed to the F^- ions located in the $d4r$ units that contain Ge-O-Ge pairs, in which no Ge has three Ge atoms as its next nearest neighbours. This may mainly correspond to $d4r$ units with a composition of $\text{Si}_{5.0}\text{Ge}_{3.0}$ or $\text{Si}_{4.0}\text{Ge}_{4.0}$.^[25,26] ^{29}Si solid-state MAS NMR spectroscopic analysis shows that all of the Si atoms in the framework are four coordinated, because of a resonance band centered at -110.2 ppm in the spectrum (Figure S4).^[27] The SPXD pattern of calcined SCM-15 shows that it is thermally stable with maintained crystalline and framework structure (Figure S5). Besides SCM-14, a small amount of GeO_2 was also detected after calcination, which may be generated from the amorphous species during the calcination (Figure S5). N_2 adsorption of calcined SCM-15 reveals the microporous nature of this material (Figure S6). The BET surface area is $395\text{ m}^2\text{ g}^{-1}$ with a micropore volume of $0.141\text{ cm}^3\text{ g}^{-1}$. Meanwhile, a bimodal pore size distribution centered at 0.60 and 0.70 nm appeared (Figure S7), which indicates a channel system with large and medium pores may be present in the structure of SCM-15.^[28]

To determine the structure of SCM-15, SCED data were collected on a typical crystal of as-made SCM-15 using the continuous rotation method (insert in Figure 1 a). The data could be indexed using the program XDS with a C-centered orthorhombic cell of $a = 25.83\text{ \AA}$, $b = 27.38\text{ \AA}$, and $c = 12.92\text{ \AA}$ (Table S2).^[29] The reconstructed reciprocal lattice in Figure 1 shows only sharp reflections, indicating that there is no disorder in the framework of SCM-15. From the reflection conditions presented in Figure 1, the possible space groups were deduced to be $Cmmm$, $Cmm2$, or $C222$. The completeness of the SCED data in the mmm Laue class remains as high as 83.5% with a resolution of 0.75 \AA , suggesting the good quality of the SCED data (Table S2). With this SCED data, the structure model of SCM-15 was first solved in the space group $Cmmm$ by the FOCUS software, and then the same structure models were also determined using Sir2014 and SHELXT.^[30–32] All of the 10 symmetrically independent framework T atoms (Si, Ge) together with 25 bridging O atoms were directly located. The struc-

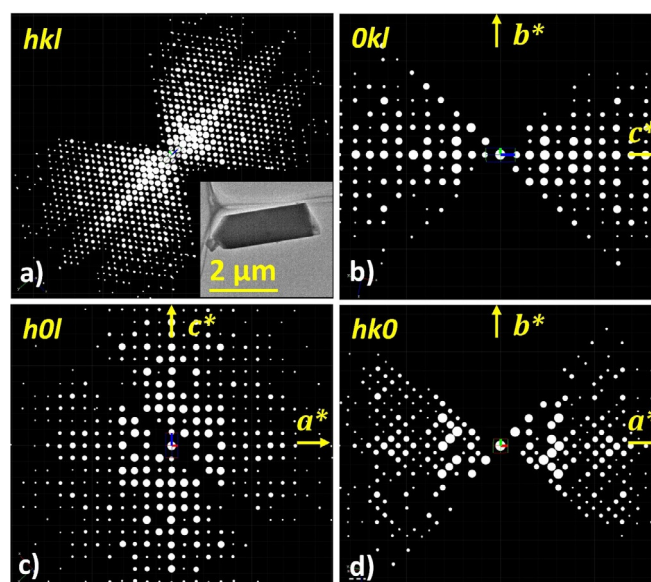


Figure 1. a) 3D reciprocal lattice of SCM-15 reconstructed from the SCED data. The crystal from which the SCED data was collected is shown in the insert. The reflection conditions deduced from the 3D reciprocal lattice and the three 2D slices b) $0kl$, c) $h0l$, and d) $hk0$ are $hkl: h+k=2n$, $0kl: k=2n$, $h0l: h=2n$, $hk0: h+k$, and $h00: h=2n$. The possible space groups are $Cmmm$, $Cmm2$, or $C222$.

ture model was initially refined against the SCED data using the program SHELXL without employing any bond and angle restraints.^[32] During the refinement, all symmetry independent T-atoms were refined as mixed Si/Ge sites, but only the T atoms located in the $d4r$ units had any significant Ge occupancy. Therefore, the other T atoms were then refined as Si. All framework atoms were refined anisotropically and an extinction correction (EXTI) was introduced to better model the low-angle reflections. The refinement converged with $R1 = 0.251$ and $wR2 = 0.515$ (Table S3, Table S4). These relatively high residuals are normal for SCED data, and are usually attributed to the multiple scattering of the electrons.

To validate the structure model determined from the SCED data and achieve a more precise framework structure and information on the location of the OSDAs, the structures of as-made and calcined SCM-15 were both refined against the SPXD using program TOPAS-V6.^[33] The geometrically optimized structure model with the space group $Cmmm$ served as a starting point for the refinement, as lowering the symmetry ($Cmm2$ and $C222$) did not provide any improvement in the refinement. Soft geometric restraints were applied on the bond distances and angles of the framework atoms. These restraints were imposed throughout the refinement, but their relative weighting with respect to the SPXD data was reduced as the refinement progressed.

For the Rietveld refinement of as-made SCM-15, an impurity phase that was identified as as-made SCM-14 was included with fixed atomic parameters.^[16] The locations of the guest species (F^- , OSDAs, and H_2O) in the framework structure of SCM-15 were elucidated using the simulated annealing algorithm as described previously.^[34] The final agreement residuals for the Rietveld refinement were $R_1 = 0.029$, $R_{wp} = 0.232$, with

$R_{\text{exp}}=0.147$ (Table 1, Figure 2). The calculated pattern matches well with the observed one, and the subtle difference can be attributed mainly to problems with the description of the peak shape. As shown in Table S5, all of the bond lengths and angles in the refined structure are in good agreement with those expected for germanosilicate zeolites. The refined phase composition is 97.5% SCM-15:2.5% SCM-14 (amorphous phase was not included), and the refined chemical composition of as-made SCM-15 is $[(\text{C}_9\text{N}_2\text{H}_{13}\text{F})_{8.0}(\text{H}_2\text{O})_{4.0}][\text{Si}_{107}\text{Ge}_{21}\text{O}_{256}]$, which corresponds well with the chemical analysis (Table S1, Figure S8). As with the SCED data, the SPXD data show that the Ge atoms are all preferentially located at the two types of symmetry independent $d4r$ units ($d4r\#1$ and $d4r\#2$), and the average compositions of these two types of $d4r$ units are $\text{Si}_{4.7}\text{Ge}_{3.3}$ for $d4r\#1$ and $\text{Si}_{6.0}\text{Ge}_{2.0}$ for $d4r\#2$, which matches well with the ^{19}F NMR spectroscopy results. For the Rietveld refinement of calcined

Table 1. Experimental and crystallographic parameters of as-made and calcined SCM-15.		
Parameters	As-made	Calcined
Composition	$[(\text{C}_9\text{N}_2\text{H}_{13}\text{F})_{8.0}(\text{H}_2\text{O})_{4.0}][\text{Si}_{107}\text{Ge}_{21}\text{O}_{256}]$	$[\text{Si}_{107}\text{Ge}_{21}\text{O}_{256}]$
Space group	<i>Cmmm</i>	<i>Cmmm</i>
a [Å]	24.8208(0)	24.8839(9)
b [Å]	26.7113(8)	26.7212(16)
c [Å]	12.7555(9)	12.6789(6)
V [Å ³]	8456.56(9)	8430.56(7)
2θ range [°]	1.8 to 35.0	1.8 to 35.0
Wavelength [Å]	0.68950	0.68950
R_i	0.029	0.027
R_{wp}	0.232	0.189
R_{exp}	0.146	0.109
Gof	1.585	1.737
Observations	9182	9182
Contributing reflections	1675	1667
Parameters	186	154
Restraints	113	113

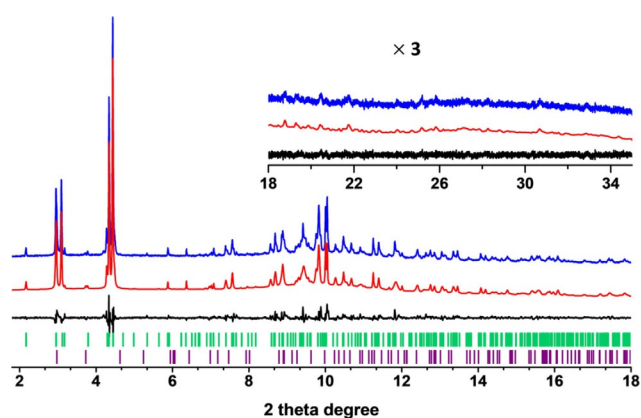


Figure 2. Structure refinement of as-made SCM-15 against the SPXD pattern. Observed (blue line), calculated (red line), as well as difference profiles (black line) are presented. The profiles in the inset have been magnified 3 times to show more details. The green and purple tick marks under the patterns are the positions of the Bragg reflections belonging to SCM-15 and SCM-14, respectively.

SCM-15, calcined SCM-14 and GeO_2 impurity phases were also included with fixed atomic parameters.^[16] The final agreement residuals of the Rietveld refinement were $R_i=0.027$, $R_{\text{wp}}=0.189$, with $R_{\text{exp}}=0.109$ (Table 1, Figure S9), and the refined chemical composition of calcined SCM-15 is $[\text{Si}_{107}\text{Ge}_{21}\text{O}_{256}]$, which also corresponds well with the chemical analysis (Table S1, Figure S8), and closely matches the calculated chemical composition of the as-made product. The framework bond lengths and angles of the refined structure are listed in Table S6.

Figure 3 shows the projections of the framework structure of SCM-15 and its channel distribution. The 3D $12\times 12\times 10$ -ring channel system of SCM-15 is constructed from three different straight channels. The two types of straight 12-ring channels along the a - and c -axes are perpendicular to each other in the ac plane, while the straight 10-ring channels lies along the b -axis.

The 10-ring channel forms 12-ring cavities at the intersection with the two 12-ring channels. The quite open structure gives SCM-15 a framework density of $15.2\text{ T}/1000\text{ \AA}^3$. To the best of our knowledge, it is the first discovered zeolite with 3D interconnected $12\times 12\times 10$ -ring channels. The effective pore sizes of the 12-ring channels along the a - and c -axes are 6.1×7.2 and $6.1\times 7.4\text{ \AA}$, respectively, while the 10-ring channels along the b -axis have openings of $5.2\times 5.9\text{ \AA}$ (taking into account an oxygen radius of 1.35 \AA). These pore sizes are somewhat similar with those observed in 3D large pore materials like *BEA ($6.6\times 7.7\text{ \AA}$) and FAU (7.4 \AA) type zeolites and 3D medium pore materials like MFI ($5.3\times 5.6\text{ \AA}$) type zeolite. Meanwhile, the pore sizes of these channels are in good agreement with the results obtained from the N_2 adsorption isotherms. It is worth noting that the unique channel system with intersecting large and medium pores may guarantee SCM-15 great potential to be applied in catalysis, since medium and large pore zeolites

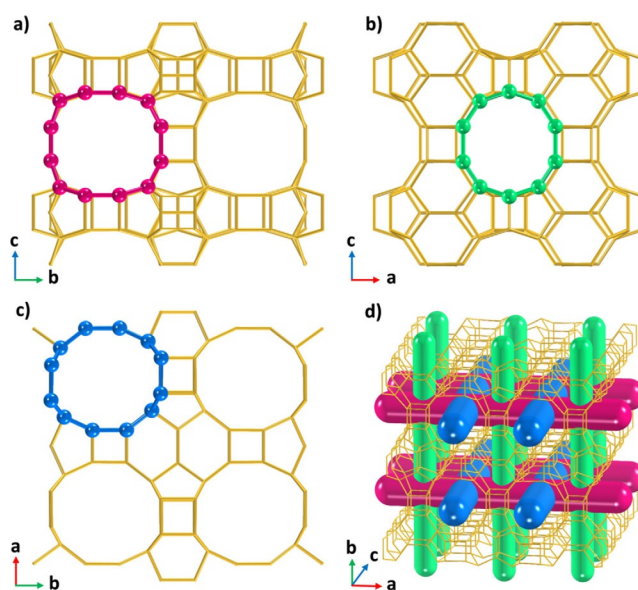


Figure 3. Projections of the framework of SCM-15 along a) [100], b) [010], and c) [001] and d) the distribution of different channels. O atoms have been omitted for clarity.

such as TON, FER, MFI, MOR, *BEA, and FAU are already widely applied in petrochemical industry and dominate the commercial market of zeolite catalysts.^[3,6] The locations of OSDAs in the framework structure can be found in Figure S10. The OSDAs (OSDA#1 and #2) are located at two symmetry independent sites in order to fit the channels with different diameters. OSDA#1 is located in the 12-ring channels, and OSDA#2 is incorporated in the 10-ring channels.

The framework structure of SCM-15 can be described by chains (referred to as SCM-15 chain) running along the *a*-axis which are interconnected through shared *d4r* units (Figure 4).

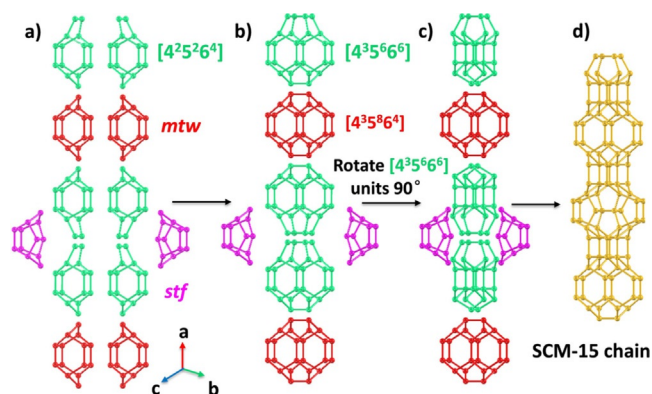


Figure 4. Construction of the SCM-15 chain. (a) Arrayed *stf*, *mtw*, and $[4^2 5^2 6^4]$ (*cbu#1*) building units, (b) two *mtw* units and two *cbu#1* units fuse together simultaneously and form $[4^3 5^8 6^4]$ (*double-mtw*) and $[4^3 5^6 6^4]$ (*cbu#2*) building units, respectively, (c,d) *cbu#2* units rotate 90° around the *a*-axis and connect together with the *double-mtw* and *stf* units to form the SCM-15 chain. O atoms have been omitted for clarity.

The SCM-15 chain is constructed by $[4^3 5^4 6^8]$ (*double-mtw*), $[4^3 5^8 6^4]$ (*cbu#2*), and *stf* units in an ordered arrangement. In turn, the *double-mtw* and *cbu#2* secondary units are formed from the *mtw* and $[4^2 5^2 6^4]$ (*cbu#1*) primary units, respectively (Figure 4a–d). In the framework structure, SCM-15 chains are arrayed with a shift along the *a*-axis and then connected through shared *d4r* units to form a layer (referred to as SCM-15 layer) with 12-ring pores along the *c*-axis (Figure 5a–c). These layers are then further connected through shared *d4r* units in the *ab* plane, forming straight 12-ring channels along the *a*- and *c*-axes and 10-ring channels along the *b*-axis (Figure 5d,e). When describing the framework structure of SCM-15 as an assimilation of chains and *d4r* units, the framework structure of SCM-15 is closely related to that of FOS-5 (BEC), ITQ-7 (ISV), PKU-16 (POS), ITQ-26 (IWS), ITQ-21, Beta polymorph B, and SU-78B, since this class of framework structures can all be built with similar chains that are further connected through shared 4-ring or *d4r* units to form straight channels (Figure S11). Meanwhile, these similar chains are also formed by similar building units (Figure S12). Inspired by the construction manners of these framework structures, six topological reasonable hypothetical zeolites, referred to as Beta-H1, Beta-H2, POS-H1, SCM-15-H1, IWS-H1, and IWS-H2 were predicted (Figure S13–S30, details can be found in the supporting information). These predicted topologically reasonable hypothetical zeolites are promising candidates for rational synthesis.

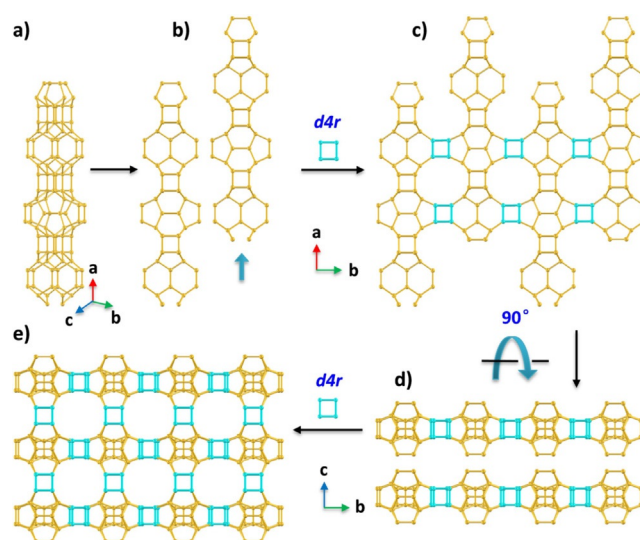


Figure 5. Assimilation of the framework structure of SCM-15 from the chains. a) SCM-15 chain, b,c) SCM-15 chains are arrayed together with a shift along *a*-axis and then connected through shared *d4r* units to build the SCM-15 layer, d,e) Neighbouring SCM-15 layers are connected together through shared *d4r* units and to form the framework structure of SCM-15. O atoms have been omitted for clarity.

In conclusion, we have demonstrated the synthesis and structure determination of SCM-15, the first 3D large pore zeolite containing interconnected $12 \times 12 \times 10$ -ring channels. The framework structure of SCM-15 has been determined from SCED data, and refined against SPXD data. The good thermal stability and the unique framework structure with interconnected large and medium pores may give SCM-15 great potential for catalytic and adsorptive applications. Meanwhile, it was found that the framework structure of SCM-15 is related to a class of framework structures that can be built from similar chains which are connected by shared 4-ring or *d4r* units. Six topologically reasonable 3D large or extra-large pore hypothetical zeolites are then predicted based on the relationship between those frameworks, and attempts to the rational synthesis of these hypothetical zeolites is underway by our group.

Experimental Section

Synthesis of SCM-15

Germanosilicate zeolite SCM-15 was synthesized using 4-pyrrolidinopyridine (OSDA, 98.0%, Shanghai Di Bo chemical technology Co., Ltd) as OSDA in fluoride medium. In a typical synthesis procedure, GeO_2 (99.0%, Sinopharm Chemical Reagent Co., Ltd) and 4-pyrrolidinopyridine were firstly added and dissolved in distilled water under stirring, and then Ludox (SiO_2 , HS-40, 40% in water, Sigma–Aldrich) was added dropwise resulting in homogeneous gel. HF (40% in water solution, Sinopharm Chemical Reagent Co., Ltd) was finally introduced to give the gel with a stoichiometry of $1 \text{SiO}_2 \cdot 0.2 \text{GeO}_2 \cdot 0.6 \text{OSDA} \cdot 0.6 \text{HF} \cdot 10 \text{H}_2\text{O}$. The gel was crystallized in a 23 mL Teflon-lined stainless-steel autoclave at 170°C for 6 days under static condition. After crystallization, the solid product was washed and dried to get the as-made SCM-15. Calcined SCM-15

was obtained after removing the guest molecules in the framework by calcination (550 °C, 5 hours) in air atmosphere.

Characterization

SCED data on as-made SCM-15 were collected using the continuous rotation method (cRED) as described previously.^[35] Data were collected on a typical crystal of SCM-15 using a JEOL JEM2100 TEM (LaB6 filament) operating at 200 kV. The goniometer was tilted from -45.00 to 65.40° with an oscillation angle of 0.184° and exposure time of 0.4 s per frame. The reciprocal space reconstruction was carried out using the program REDp,^[36] and the reflection intensity extraction was conducted by the program XDS.^[29] SPXD data were collected on an as-made and calcined sample of SCM-15 in a 0.5 mm capillary on the BL14B1 beamline ($\lambda = 0.68950 \text{ \AA}$) at the Shanghai Synchrotron Radiation Facility in Shanghai, China. The collected data were ranging from 1.8 to 35.0° with 0.004° data binning.

Characterization of the crystal morphology and energy-dispersive X-ray spectroscopy (EDS) analyses were performed using a field emission XL30E scanning electron microscopy (SEM, FEI Company) equipped with an EDAX Phoenix EDS Detector. ^{29}Si solid-state MAS NMR spectra were acquired on a Varian Model VNMRS-400WB spectrometer with a 7.5 mm probe at 79.43 MHz and a spinning rate of 3 kHz. ^{13}C liquid NMR spectra (recorded on a Bruker AV-400 spectrometer) and solid-state MAS NMR spectra (recorded on a Varian Model VNMRS-400WB spectrometer with a 7.5 mm probe at 100.54 MHz and a spinning rate of 5 kHz) were both collected to figure out the state of OSDAs. ^{19}F solid-state NMR spectra were recorded on a Bruker AVANCEIII 500WB spectrometer with a 2.5 mm probe at 376.5 MHz with a spinning rate of 30 kHz. The molar ratios of Si/Ge were also quantified by inductively coupled plasma emission spectrometry (ICP) on a Varian 725-ES instrument after dissolving the sample in HF solution. Elemental analyses of C, N, and H were conducted on an ElementarVario MICRO CUBE elemental analyzer. Nitrogen adsorption experiments were performed on a MICROMERITICS ASAP2010 Accelerated Surface Area & Porosimetry System. The DSC-TGA curves were collected on a SDT Q600 V20.9 Build 20 thermal analyzer. Samples were exposed to air atmosphere where temperature was elevated from 30 to 900 °C at a rate of $10^\circ\text{C min}^{-1}$.

Acknowledgements

The authors gratefully acknowledge Dr. Jianqiang Wang and the beamline scientists (beamline BL14B1 at the SSRF, Shanghai, China) for their assistance with the SPXD experiments. The authors acknowledge financial support from the National Key R&D Program of China (project number: 2017YFB0702800), China Petrochemical Corporation (Sinopec Group), the National Natural Science Foundation of China (project numbers: 21503280, 21527803, 21471009, 2162106), and the Swiss National Science Foundation (project number: 177761).

Conflict of interest

The authors declare no conflict of interest.

Keywords: channel system • organic structure-directing agent • structure determination • synthetic methods • zeolites

- [1] M. E. Davis, *Nature* **2002**, *417*, 813–821.
- [2] M. E. Davis, *Chem. Mater.* **2014**, *26*, 239–245.
- [3] W. Vermeiren, J.-P. Gilson, *Top. Catal.* **2009**, *52*, 1131–1161.
- [4] L. Tosheva, V. P. Valtchev, *Chem. Mater.* **2005**, *17*, 2494–2513.
- [5] R. F. Lobo, S. I. Zones, M. E. Davis, *J. Inclusion Phenom. Mol. Recognit. Chem.* **1995**, *21*, 47–78.
- [6] S. I. Zones, *Microporous Mesoporous Mater.* **2011**, *144*, 1–8.
- [7] T. Willhammar, J. Sun, W. Wan, P. Oleynikov, D. Zhang, X. Zou, M. Moliner, J. Gonzalez, C. Martínez, F. Rey, A. Corma, *Nat. Chem.* **2012**, *4*, 188–194.
- [8] R. F. Lobo, M. E. Davis, *J. Am. Chem. Soc.* **1995**, *117*, 3766–3779.
- [9] C. Baerlocher, L. B. McCusker, *Database of Zeolite Structures*, <http://europa.izastructure.org/IZA-SC/framework.php?STC=CON>.
- [10] C. Baerlocher, L. B. McCusker, *Database of Zeolite Structures*, http://europa.iza-structure.org/IZA-SC/material_tm.php?STC=IWR.
- [11] P. A. Wright, R. H. Jones, S. Natarajan, R. G. Bell, J. Chen, M. B. Hursthouse, J. M. Thomas, *J. Chem. Soc. Chem. Commun.* **1993**, 633–635.
- [12] M. Moliner, T. Willhammar, W. Wan, J. González, F. Rey, J. L. Jorda, X. Zou, A. Corma, *J. Am. Chem. Soc.* **2012**, *134*, 6473–6478.
- [13] Y. Lorgouilloux, M. Dodin, E. Mugnaioli, C. Marichal, P. Caullet, N. Bats, U. Kolb, J.-L. Paillaud, *RSC Adv.* **2014**, *4*, 19440–19449.
- [14] D. L. Dorset, S. C. Weston, S. S. Dhingra, *J. Phys. Chem. B* **2006**, *110*, 2045–2050.
- [15] M. Dodin, J.-L. Paillaud, Y. Lorgouilloux, P. Caullet, E. Elkaim, N. Bats, *J. Am. Chem. Soc.* **2010**, *132*, 10221–10223.
- [16] Y. Luo, S. Smeets, F. Peng, A. S. Etman, Z. Wang, J. Sun, W. Yang, *Chem. Eur. J.* **2017**, *23*, 16829–16834.
- [17] J. Simancas, R. Simancas, P. J. Bereciartua, J. L. Jorda, F. Rey, A. Corma, S. Nicolopoulos, P. P. Das, M. Gemmi, E. Mugnaioli, *J. Am. Chem. Soc.* **2016**, *138*, 10116–10119.
- [18] T. Conradsson, M. S. Dadachov, X. D. Zou, *Microporous Mesoporous Mater.* **2000**, *41*, 183–191.
- [19] L. A. Villaescusa, P. A. Barrett, M. A. Cambor, *Angew. Chem. Int. Ed.* **1999**, *38*, 1997–2000; *Angew. Chem.* **1999**, *111*, 2164–2167.
- [20] W. Hua, H. Chen, Z.-B. Yu, X. Zou, J. Lin, J. Sun, *Angew. Chem. Int. Ed.* **2014**, *53*, 5868–5871; *Angew. Chem.* **2014**, *126*, 5978–5981.
- [21] D. L. Dorset, K. G. Strohmaier, C. E. Kiewer, A. Corma, M. J. Díaz-Cabañas, F. Rey, C. J. Gilmore, *Chem. Mater.* **2008**, *20*, 5325–5331.
- [22] A. Corma, M. J. Díaz-Cabañas, J. Martínez-Triguero, F. Rey, J. Rius, *Nature* **2002**, *418*, 514–517.
- [23] J. M. Newsam, M. M. J. Treacy, W. T. Koetsier, C. B. D. Gruyter, *Proc. R. Soc. London Ser. A* **1988**, *420*, 375–405.
- [24] Z.-B. Yu, Y. Han, L. Zhao, S. Huang, Q.-Y. Zheng, S. Lin, A. Córdova, X. Zou, J. Sun, *Chem. Mater.* **2012**, *24*, 3701–3706.
- [25] A. Pulido, G. Sastre, A. Corma, *ChemPhysChem* **2006**, *7*, 1092–1099.
- [26] R. T. Rigo, S. R. G. Balestra, S. Hamad, R. Bueno-Perez, A. R. Ruiz-Salvador, S. Calero, M. A. Cambor, *J. Mater. Chem. A* **2018**, *6*, 15110–15122.
- [27] T. Blasco, A. Corma, M. J. Díaz-Cabañas, F. Rey, J. A. Vidal-Moya, C. M. Zicovich-Wilson, *J. Phys. Chem. B* **2002**, *106*, 2634–2642.
- [28] C.-Y. Chen, L. W. Finger, R. C. Medrud, C. L. Kibby, P. A. Crozier, I. Y. Chan, T. V. Harris, L. W. Beck, S. I. Zones, *Chem. Eur. J.* **1998**, *4*, 1312–1323.
- [29] W. Kabsch, *Acta Crystallogr. Sect. D* **2010**, *66*, 125–132.
- [30] S. Smeets, L. B. McCusker, C. Baerlocher, E. Mugnaioli, U. Kolb, *J. Appl. Crystallogr.* **2013**, *46*, 1017–1023.
- [31] M. C. Burla, R. Caliendo, B. Carrozzini, G. L. Cascarano, C. Cuocci, C. Giacovazzo, M. Mallamo, A. Mazzzone, G. Polidori, *J. Appl. Crystallogr.* **2015**, *48*, 306–309.
- [32] G. M. Sheldrick, *Acta Crystallogr. Sect. A* **2008**, *64*, 112–122.
- [33] A. A. Coelho, *J. Appl. Crystallogr.* **2018**, *51*, 210–218.
- [34] S. Smeets, L. B. McCusker, C. Baerlocher, S. Elomari, D. Xie, S. I. Zones, *J. Am. Chem. Soc.* **2016**, *138*, 7099–7106.
- [35] Y. Wang, S. Takki, O. Cheung, H. Xu, W. Wan, L. Öhrström, A. K. Inge, *Chem. Commun.* **2017**, 53, 7018–7021.
- [36] W. Wan, J. Sun, J. Su, S. Hovmöller, X. Zou, *J. Appl. Crystallogr.* **2013**, *46*, 1863–1873.

Manuscript received: October 15, 2018

Accepted manuscript online: December 6, 2018

Version of record online: January 14, 2019